

# Effect of Humidity on the Adsorption Kinetics of Lung Surfactant at Air–Water Interfaces

Yi Y. Zuo,<sup>†</sup> Roya Gitiafroz,<sup>‡</sup> Edgar Acosta,<sup>‡</sup> Zdenka Policova,<sup>†</sup> Peter N. Cox,<sup>§</sup> Michael L. Hair,<sup>†</sup> and A. Wilhelm Neumann<sup>\*,†</sup>

Department of Mechanical and Industrial Engineering, University of Toronto, 5 King's College Road, Toronto, Ontario, M5S 3G8 Canada, Department of Chemical Engineering and Applied Chemistry, University of Toronto, 200 College Street, Toronto, Ontario, M5S 3E5 Canada, and Department of Critical Care Medicine, The Hospital for Sick Children, 555 University Avenue, Toronto, Ontario, M5G 1X8 Canada

Received June 24, 2005. In Final Form: August 4, 2005

The in vitro adsorption kinetics of lung surfactant at air–water interfaces is affected by both the composition of the surfactant preparations and the conditions under which the assessment is conducted. Relevant experimental conditions are surfactant concentration, temperature, subphase pH, electrolyte concentration, humidity, and gas composition of the atmosphere exposed to the interface. The effect of humidity on the adsorption kinetics of a therapeutic lung surfactant preparation, bovine lipid extract surfactant (BLES), was studied by measuring the dynamic surface tension (DST). Axisymmetric drop shape analysis (ADSA) was used in conjunction with three different experimental methodologies, i.e., captive bubble (CB), pendant drop (PD), and constrained sessile drop (CSD), to measure the DST. The experimental results obtained from these three methodologies show that for 100% relative humidity (RH) at 37 °C the rate of adsorption of BLES at an air–water interface is substantially slower than for low humidity. It is also found that there is a difference in the rate of surface tension decrease measured from the PD and CB/CSD methods. These experimental results agree well with an adsorption model that considers the combined effects of entropic force, electrostatic interaction, and gravity. These findings have implications for the development and evaluation of new formulations for surfactant replacement therapy.

## 1. Introduction

Lung surfactant is a complicated mixture of approximately 90% lipids and 10% proteins.<sup>1</sup> Its main function is to reduce the surface tension of the alveolar surface.<sup>2</sup> This ability plays an important role in maintaining the normal mechanics of respiration.<sup>3</sup> By lowering alveolar surface tension, first, the amount of energy required to inflate the lungs is reduced due to increased lung compliance; second, the likelihood of lung collapse during expiration is reduced by decreasing elastic recoil. As a result, the lungs can easily maintain patency by a small transpulmonary pressure.<sup>4</sup>

Respiratory distress syndrome (RDS) is a major disease of lung surfactant deficiency worldwide.<sup>5,6</sup> Patients with RDS are premature infants who exhibit increased work of breathing, decreased lung compliance, prominent atelectasis with reduced function residual capacity, impaired gas exchange, and diffused interstitial edema.<sup>5</sup> As

many as 50 000–60 000 premature infants in the United States alone are threatened by RDS annually.<sup>5</sup>

Exogenous surfactant replacement therapy, in which either synthetic or natural lung surfactants extracted from mammalian lungs are delivered to the patients, has been used as a standard therapeutic intervention for patients with RDS.<sup>7</sup> A primary necessity of these exogenous surfactants, analogous to the endogenous surfactant, is that they must adsorb rapidly to the air–liquid interface of the alveoli, within the period of a single breath (i.e., a few seconds).<sup>8</sup>

The process of adsorption is usually studied by measuring dynamic surface tension (DST), i.e., the time-dependent surface tension which corresponds to the adsorption kinetics. The general correlation between the adsorption process and DST decrease has been reviewed previously.<sup>9,10</sup> The adsorption of lung surfactant to an air–water interface is indicated by the decrease of DST from the air–water value (i.e.,  $\sim 70$  mJ/m<sup>2</sup> at 37 °C) to the equilibrium value of a predominantly phospholipid film (i.e., 22–25 mJ/m<sup>2</sup>).<sup>1</sup>

The in vitro adsorption of lung surfactant is apparently dependent on both the composition of these surfactants and the conditions under which they are assessed. Numerous efforts have been made to study the effects of different surfactant compositions on the adsorption behavior. These studies investigate the adsorption of both

\* To whom correspondence should be addressed. Tel.: +1-416-978-1270. Fax: +1-416-978-7753. E-mail: neumann@mie.utoronto.ca.

<sup>†</sup> Department of Mechanical and Industrial Engineering, University of Toronto.

<sup>‡</sup> Department of Chemical Engineering and Applied Chemistry, University of Toronto.

<sup>§</sup> The Hospital for Sick Children.

(1) Possmayer, F. In *Fetal and Neonatal Physiology*, 2nd ed; Polin, R. A., Fox, W. W., Eds.; WB Saunders Company: Philadelphia, 1992; p 949.

(2) Clements, J. A. *Physiologist* **1962**, *5*, 11.

(3) Zasadzinski, J. A.; Ding, J.; Warriner, H. E.; Bringezu, F.; Waring, A. J. *Curr. Opin. Colloid Interface Sci.* **2001**, *6*, 506.

(4) Scarpelli, E. M. *Surfactants and the Lining of the Lung*; Johns Hopkins University Press: Baltimore, 1988.

(5) Notter, R. H. *Lung Surfactant, Basic Science and Clinical Application*; Marcel Dekker: New York, 2000.

(6) Frerking, I.; Gunther, A.; Seeger, W.; Pison, U. *Intensive Care Med.* **2001**, *27*, 1699.

(7) Robertson, B.; Haliday, H. L. *Biochim. Biophys. Acta* **1998**, *1408*, 346.

(8) Goerke, J.; Clements, J. A. In *Handbook of Physiology: The Respiratory System*; Macklem, P. T., Mead J., Eds.; American Physiology Society: Bethesda, MD, 1986; p 247.

(9) Chang S.-H.; Franses, E. I. *Colloids and Surfaces A: Physicochem. Eng. Aspects* **1995**, *100*, 1.

(10) Fainerman, V. B.; Miller, R.; Möhwald, H. *J. Phys. Chem. B.* **2002**, *106*, 809.

naturally extracted lung surfactants<sup>11,12</sup> and their prime components/mixtures, e.g., dipalmitoyl phosphatidylcholine (DPPC),<sup>13,14</sup> DPPC/dipalmitoyl phosphatidylglycerol (DPPC/DPPG) mixtures,<sup>15</sup> surfactant associated proteins,<sup>16</sup> surfactant extracted lipids/proteins mixtures,<sup>17–19</sup> and even the less abundant components such as cholesterol.<sup>20</sup> To aim at developing new formulations for the surfactant replacement therapy, the studies of composition are also extended to potential alternatives or additives that may act as artificial surfactants, such as peptidolipid mixtures,<sup>21</sup> dilauroyl phosphatidylcholine (DLPC),<sup>22</sup> and nonionic polymers.<sup>23,24</sup>

The effects of experimental conditions on the adsorption of lung surfactants or their primary components have also been studied. These experimental conditions are mainly surfactant concentration,<sup>25</sup> temperature,<sup>26</sup> size of the dispersed particles (which is mainly dependent on the preparation protocol),<sup>14,22</sup> pH and electrolyte concentration of the subphase,<sup>27–32</sup> humidity,<sup>33,34</sup> and composition<sup>35</sup> of the gas exposed to the surfactant film.

Influencing factors, except for concentration and temperature, are relatively poorly understood, especially the effect of humidity. Nearly 30 years ago, Colacicco et al.<sup>33</sup> first addressed the effect of humidity on the surface activity of DPPC films. They found that the surface activity of both spreading and adsorbed DPPC films was significantly impaired by 100% relative humidity (RH) at 37 °C. For instance, when the atmosphere above an adsorbed DPPC film (formed in a Langmuir trough) was presaturated with water vapor at 37 °C, the minimum surface tension that could be reached by 20% film compression was merely 22 mJ/m<sup>2</sup>. In contrast, a near zero surface tension could be easily obtained by the same compression but keeping the atmosphere dry. They drew the conclusion that the high

humidity destabilized the DPPC films, perhaps by hydration of these films from the air side of the interfacial film.<sup>33</sup>

A similar effect of humidity on lung surfactant extracts was also reported by Wildeboer-Venema.<sup>34</sup> Using lavage from dogs' lungs, Wildeboer-Venema found that at 37 °C, 100% RH did not affect the equilibrium surface tension of the adsorbed lung surfactant films but decreased their dynamic stability, i.e., increased the minimum surface tension upon compression. He speculated that the decrease in film stability might be due to the penetration of water molecules through the fatty acid chains of the phospholipid film and the interaction of these water molecules with the polar headgroups of the phospholipids forming the film.

These pioneering studies found little attention in the last 25 years. Nevertheless, if the humidity does play a role in the surface activity of lung surfactant films, it deserves further investigation as the alveolar gas is well-known to be saturated with water.<sup>36,37</sup> Consequently, the in vitro assessment of lung surfactants, especially those preparations for surfactant replacement therapy, should be conducted at an atmosphere with 100% RH at 37 °C, i.e., in close simulation of the in vivo environment.

The effect of humidity on the adsorption kinetics of a therapeutic lung surfactant, bovine lipid extract surfactant (BLES), is studied in this paper. BLES is a mixture of phospholipids and lung surfactant associated protein B (SP-B) and C (SP-C). The DST, indicating the adsorption kinetics, is measured by a drop shape technique, called axisymmetric drop shape analysis (ADSA). Three different experimental methodologies, captive bubble (CB), pendant drop (PD), and constrained sessile drop (CSD), are used in conjunction with ADSA to demonstrate the effects of humidity. The results from these different experimental methodologies, to be presented below, show remarkable consistency and show impeded adsorption in "wet" conditions compared with "dry" conditions. Further comparison of the adsorption rate measured from these three different arrangements indicates a primary difference in the adsorption mechanism between CB/CSD and PD configurations. These experimental results fit an adsorption model which considers a combined effect of entropic force, electrostatic interaction, and gravity. The findings have implications in developing and evaluating new formulations for the surfactant replacement therapy.

## 2. Materials and Methods

**2.1. Materials.** The lung surfactant used in this study is BLES (BLES Biochemicals Inc, London, ON, Canada). BLES is a therapeutic surfactant and is commercially available. It is prepared by organic extraction from bronchopulmonary bovine lung lavage. BLES contains about 98% phospholipids (45% dipalmitoyl phosphatidylcholine (DPPC), 35% unsaturated phosphatidylcholines (PCs), 12% phosphatidylglycerol (PG), 2% phosphatidylethanolamine (PE), 1% phosphatidylinositol (PI), 1% lysophosphatidylcholine (LPC), 2% sphingomyelin (SPH)) and 2% proteins. Among these phospholipids, the headgroups of PC, PE, and SPH compounds are zwitterionic; those of PG and PI compounds are anionic (Notter, 2000). The protein components in BLES are only SP-B and SP-C. High molecular weight hydrophilic proteins, SP-A and SP-D, have been removed during the extraction with organic solvents. BLES is stored frozen in sterilized vials with an initial concentration of 27 mg/mL. It is diluted to 0.5 mg/mL by a salt solution of 0.6% NaCl and 1.5 mM CaCl<sub>2</sub> on the day of the experiment. The water used in the experiments is demineralized and glass distilled. The pH of the diluted BLES preparations was found to be 5.6.

(11) Notter, R. H.; Finkelstein, J. N.; Taubold, R. D. *Chem. Phys. Lipids* **1983**, *33*, 67.

(12) Park, S. Y.; Hannemann, R. E.; Franses, E. I. *Colloids Surf. B: Biointerfaces* **1999**, *15*, 325.

(13) Chu, J.; Clements, J. A.; Cotton, E. K.; Klaus, M. H.; Sweet, A. Y.; Tooley, W. H.; Bradley, B. L.; Brandorff, L. C. *Pediatrics* **1967**, *40*, 709.

(14) Wen, X.; Franses, E. I. *Langmuir* **2001**, *17*, 3194.

(15) Ross, M.; Krol, S.; Janshoff, A.; Galla, H. J. *Eur. Biophys. J.* **2002**, *31*, 52.

(16) Taneva, S. G.; Keough, K. M. W. *Biochemistry* **2000**, *39*, 6083.

(17) Walters, R. W.; Jeng, R. R.; Hall, S. B. *Biophys. J.* **2000**, *78*, 257.

(18) Schram, V.; Hall, S. B. *Biophys. J.* **2001**, *81*, 1536.

(19) Schram, V.; Walter, R. A.; Hall, S. B. *Biochim. Biophys. Acta* **2003**, *1616*, 165.

(20) Yu, S. H.; Possmayer, F. *J. Lipid Res.* **2001**, *42*, 1421.

(21) Palmblad, M.; Gustafsson, M.; Curstedt, T.; Johansson, J.; Schürch, S. *Biochim. Biophys. Acta* **2001**, *1510*, 106.

(22) Pinazo, A.; Wen, X.; Liao, Y.-C.; Prosser, A. J.; Franses, E. I. *Langmuir* **2002**, *18*, 8888.

(23) Taeusch, H. W.; Lu, K. W.; Goerke, J.; Clements, J. A. *Am. J. Respir. Crit. Care Med.* **1999**, *159*, 1391.

(24) Yu, L. M. Y.; Lu, J. J.; Chiu, I. W. Y.; Leung, K. S.; Chan, Y. W.; Zhang, L.; Policova, Z.; Hair, M. L.; Neumann, A. W. *Colloids Surf. B: Biointerfaces* **2004**, *36*, 167.

(25) Lu, J. J.; Yu, L. M. Y.; Cheung, W. W. Y.; Policova, Z.; Li, D.; Hair, M. L.; Neumann, A. W. *Colloids Surf. B: Biointerfaces* **2003**, *29*, 119.

(26) Goerke, J.; Gonzales, J. *J. Appl. Physiol.* **1981**, *51*, 1108.

(27) Scarpelli, E. M.; Gabbay, K. H.; Kochen, J. A. *Science* **1965**, *148*, 1607.

(28) Davies, R. J.; Genghini, M.; Walters, D. V.; Morley, C. J. *Biochim. Biophys. Acta* **1986**, *878*, 135.

(29) Haddad, I. Y.; Holm, B. A.; Hlavaty, L.; Matalon, S. *J. Appl. Physiol.* **1994**, *76*, 657.

(30) Amirkhani, J. D.; Merritt, T. A. *Lung* **1995**, *173*, 243.

(31) Camacho, L.; Cruz, A.; Castro, R.; Casals, C.; Pérez-Gil, J. *Colloids Surf. B: Biointerfaces* **1996**, *5*, 217.

(32) Phang, T.-L.; Liao, Y.-C.; Franses, E. I. *Langmuir* **2004**, *20*, 4004.

(33) Colacicco, G.; Basu, M. K.; Scarpelli, E. M. *Respir. Physiol.* **1976**, *27*, 169.

(34) Wildeboer-Venema, F. *Respir. Physiol.* **1980**, *39*, 63.

(35) Wildeboer-Venema, F. *Respir. Physiol.* **1984**, *58*, 1.

(36) Christie, R. V.; Loomis, A. L. *J. Physiol. (London)* **1932**, *77*, 35.

(37) Fox, S. I. *Human Physiology*, 6th ed.; McGraw-Hill: New York, 1999.

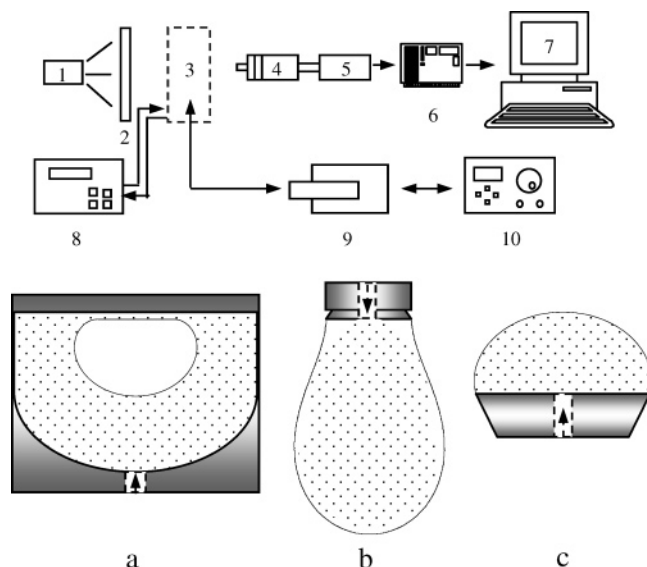


**Figure 1.** Schematic of the experimental setup and the three different drop/bubble configurations. (a) Captive bubble (CB); (b) pendant drop (PD); (c) constrained sessile drop (CSD). The arrows in the different drop/bubble configurations show the directions of the fluid flow. 1. Light source; 2. diffuser; 3. thermostated drop/bubble cell; 4. microscope; 5. CCD camera; 6. digital video processor; 7. workstation; 8. water bath; 9. motorized syringe; 10. motor controller.

**2.2. Methods. 2.2.1. ADSA.** ADSA is a surface tension measurement methodology based on the shape of drops or bubbles. It was first introduced by Rotenberg et al.<sup>38</sup> and has been continuously improved in the last two decades.<sup>39–42</sup> Conceptually, ADSA determines surface tension by numerically fitting the shape of experimental drops/bubbles to theoretical profiles given by the classical Laplace equation of capillarity. The only assumptions made in ADSA are that the drops/bubbles are Laplacian and axisymmetric. Input parameters of ADSA are the local gravitational acceleration, the density difference across the interface, and a number of coordinates of the drop/bubble profile automatically detected by digital image analysis. Typical output of ADSA includes surface tension, contact angle, drop/bubble superficial area and volume, and curvature of the drop/bubble at the apex. Running on either UNIX workstations or IBM-compatible personal computers, ADSA features an easy-to-use interface and high processing speed (i.e., 1 to 2 s per image).<sup>41</sup> Details related to the algorithms of ADSA can be found elsewhere.<sup>39,43</sup>

**2.2.2. Experimental Setup and Protocol.** Three different experimental arrangements were used to measure DST during adsorption. A schematic of the general experimental setup and the three drop/bubble configurations, i.e., CB, PD, and CSD, are shown in Figure 1. A detailed description of these three arrangements has been given before.<sup>24,25,44,45</sup> Briefly, for PD or CSD, a drop was formed by a motor-driven syringe. The time of forming a drop was less than 0.5 s, precisely controlled by a programmable motor controller (18705/6, Oriel Instru, Stratford,

CT). This rapid drop formation ensured that the subsequent adsorption was studied at a fresh, clean air–water interface. For CB, a bubble was injected into a liquid-filled chamber by a microsyringe (50  $\mu$ L, #1705, Gastight, Hamilton Corp, Reno, NY). After injection, the bubble immediately rested against the ceiling of the chamber and formed a Laplacian shape. The whole process took less than 5 s.

Image acquisition, at a rate of 30 images per second, commenced immediately after the drop/bubble formation and lasted for 5 min. The acquired images were processed by a digital video processor (Parallax Graphics, Rocklin, CA) and stored in a workstation (Sparc Station-10, Sun Microsystems Inc., Santa Clara, CA) for further analysis by ADSA. The system temperature was thermostatically maintained by a water bath (model RTE-111, Neslab Instruments Inc, Portsmouth, NH) at 37  $^{\circ}$ C, constant within  $\pm 0.2$   $^{\circ}$ C. The entire experimental setups, except the computer, were mounted on a vibration-free table (Technical Manufacturing Corp, Peabody, MA) which was equipped with compressed air bladders to minimize random vibrations.

It should be noted that all experiments were conducted using the same surfactant preparation (i.e., BLES) under the same experimental conditions (e.g., 0.5 mg/mL BLES concentration and 37  $^{\circ}$ C) except for varying the humidity. The three drop/bubble configurations and the control of humidity in these arrangements are as follows.

**(1) CB Arrangement.** The CB arrangement used here is the same as described before.<sup>44</sup> To vary the humidity in the gas phase (i.e., the bubble), the gas used to form the bubbles was manipulated in the following way: the air used to form a “wet” bubble was presaturated with water vapor in a humidification chamber maintained at 37  $^{\circ}$ C and saturated with water (RH > 99%). The RH was measured by a hygrometer (Omega RH411 Relative Humidity Meter, CT). A “dry” bubble was formed using ambient air, at the room temperature of 25  $^{\circ}$ C and RH less than 50%. The reasons of using the ambient air rather than completely dehydrated air (i.e., RH = 0%) are (1) to make the current study comparable to those published previously where ambient air was routinely used to form a bubble;<sup>42</sup> (2) due to the difficulty in measuring and maintaining the humidity in a CB, even though completely dry air was used to form a bubble, the gas phase in the bubble would still be humidified somewhat. Therefore, ambient air was simply used here to represent the dry environment.

**(2) PD Arrangement.** Different from a previous setup,<sup>24,25</sup> the PD arrangement used here was modified as shown in Figure 1b. Instead of a conventional capillary made of Teflon or quartz, this new constellation, made of stainless steel (SS316), is an inverted pedestal with a sharp knife edge. Owing to the hydrophilicity of the material, the pedestal allows the formation of well-deformed drops, favorable for accurate surface tension measurements.

The drop was enclosed in a quartz glass cuvette (model 100-QS, Hellma), which was placed in a temperature chamber (model 100-07, Ramé–Hart). A “wet” atmosphere was produced by placing a reservoir of water in the chamber well before the experiment until the RH was more than 99%. In contrast, a “dry” atmosphere was produced by replacing the water reservoir with desiccant of anhydrous  $\text{CaSO}_4$ . The experiment was not started until the hygrometer gave a reading of 0% RH.

**(3) CSD Arrangement.** CSD is a novel drop configuration recently developed in the authors’ laboratory.<sup>45</sup> As shown in Figure 1c, a sessile drop was formed on a pedestal, which employed a horizontal sharp-knife edge to prevent the test liquid from spreading upon the solid surface at low surface tensions (film leakage). The drop and pedestal were enclosed in a temperature chamber made of stainless steel (SS316). Humidity in the chamber was controlled in the same way as in the PD arrangement.

**2.2.3. Data Processing. (1) Averaging.** DSTs measured from different experimental runs were averaged by linearly interpolating the surface tensions measured at different time points to a spectrum with a uniform interval of 10 ms. The time interval between two adjacent measurements is only 33.3 ms (i.e., 30 images/s), and therefore, linear interpolation is accurate enough to produce a smooth and unbiased sequence of data.

(38) Rotenberg, Y.; Boruvka, L.; Neumann, A. W. *J. Colloid Interface Sci.* **1983**, *93*, 169.

(39) del Río, O. I.; Neumann, A. W. *J. Colloid Interface Sci.* **1997**, *196*, 136.

(40) Hoorfar, M.; Neumann, A. W. *J. Adhesion* **2004**, *80*, 727.

(41) Zuo, Y. Y.; Ding, M.; Bateni, A.; Hoorfar, M.; Neumann, A. W. *Colloids Surfaces A: Physicochem. Eng. Aspects* **2004**, *250*, 233.

(42) Zuo, Y. Y.; Ding, M.; Li, D.; Neumann, A. W. *Biochim. Biophys. Acta* **2004**, *1675*, 12.

(43) Lahooti, S.; del Río, O. I.; Cheng, P.; Neumann, A. W. In *Applied Surface Thermodynamics*; Neumann, A. W., Spelt, J. K., Eds.; Marcel Dekker: New York, 1996; p 441.

(44) Zuo, Y. Y.; Li, D.; Acosta, E.; Cox, N. P.; Neumann, A. W. *Langmuir* **2005**, *21*, 5446.

(45) Yu, L. M. Y.; Lu, J. J.; Chan, Y. W.; Ng, A.; Zhang, L.; Hoorfar, M.; Policova, Z.; Grundke, K.; Neumann, A. W. *J. Appl. Physiol.* **2004**, *97*, 704.

**(2) First Derivative of the Experimental Data.** The rate of adsorption, i.e., the first derivative of surface tension with respect to time ( $-(d\gamma/dt)$ ), was calculated by a digital differentiator, Savitzky-Golay (SG) filter.<sup>46,47</sup> The SG filter takes the first derivative by moving a convolution mask, based on a piecewise least-squares polynomial fitting, over the experimental data.

### 3. Results

**3.1. CB Studies.** Figure 2a shows the adsorption curves of 0.5 mg/mL BLES in dry conditions, obtained from five different CB experimental runs. These runs demonstrate good reproducibility. The initial surface tensions are well below the value of a clean air–water surface, i.e., 70.1 mJ/m<sup>2</sup> at 37 °C.<sup>48</sup> These low initial surface tensions indicate rapid adsorption occurring in the interval of forming the bubble (i.e., <5 s). The adsorption curves show two distinct stages. In the first stage, up to approximately 25 s, the surface tension decreases rapidly to a value below 25 mJ/m<sup>2</sup>. In the next 275 s, the surface tension decreases slightly to an ultimate equilibrium value of approximately 24.5 mJ/m<sup>2</sup>.

Figure 2b shows the adsorption curves in wet conditions, obtained from three different CB experimental runs. Again, good reproducibility is obtained. It is noted that these curves are significantly different from their counterparts in dry conditions (Figure 2a). The adsorption in wet conditions is much slower in comparison with the dry conditions. The initial surface tensions range from 55 to 60 mJ/m<sup>2</sup>. Again, the surface tension of a clean air–water interface is not obtained due to adsorption during bubble formation. However, since the time elapsed for forming a bubble in dry and wet conditions is the same (i.e., 5 s), the pronounced difference in the initial surface tension suggests that the initial adsorption in dry conditions is much faster than in wet conditions. The adsorption curves in wet conditions also show a general two-stage shape, i.e., a surface tension decrease in the first 150–170 s, followed by a slow equilibration to a surface tension of approximately 24.2 mJ/m<sup>2</sup>. However, the time to reach equilibrium in wet conditions is approximately five times more than in dry conditions. It should also be noted (Figure 2b) that, at surface tensions near 40 mJ/m<sup>2</sup>, a “shoulder” appears in each curve, in which surface tension decrease shows a rather moderate slope. After the shoulder, the slope turns steep again, indicating an acceleration in the decrease of surface tension. This change in the rate of surface tension decrease can be clarified by studying the adsorption rate, i.e., the first derivative of surface tension decrease with respect to time, which will be discussed later.

The effect of humidity on the adsorption kinetics of BLES is more clearly presented in Figure 2c, in which the averaged adsorption curves (from those shown in Figure 2, panels a and b, respectively) in dry and wet conditions are compared. It is clear that the adsorption of BLES on the surface of a CB formed by water-saturated air is much slower than the bubble formed by ambient air. It is also noted that humidity only affects the rate of adsorption but not the equilibrium surface tension.

**3.2. PD Studies.** Figure 3a shows the adsorption curves of 0.5 mg/mL BLES in dry conditions, obtained from four different PD experimental runs. These curves are easily reproducible and similar to those obtained from CB (Figure

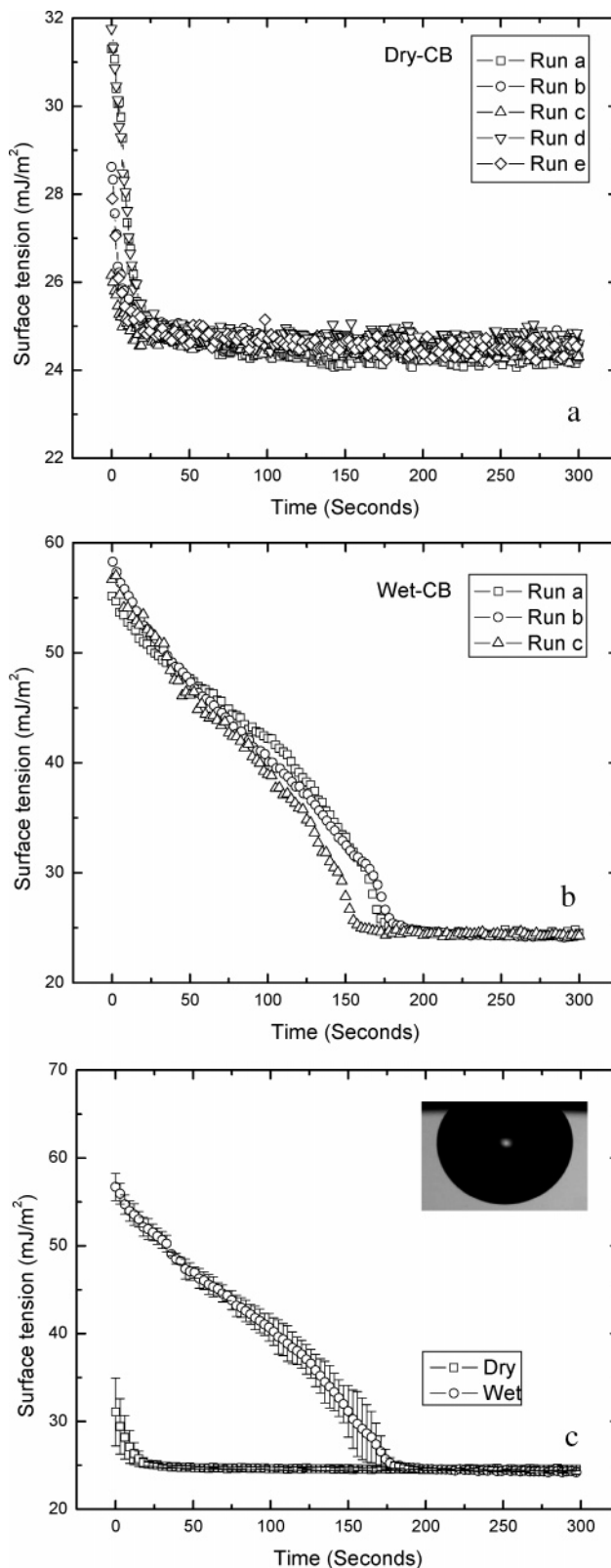


**Figure 2.** Dependence of adsorption kinetics of 0.5 mg/mL BLES on humidity, studied by a captive bubble (CB) method at 37 °C. (a) Five individual experimental runs in dry conditions; (b) three individual experimental runs in wet conditions; (c) averaged adsorption curves in dry and wet conditions. The error bar shows the standard deviation of the average.

2a). Figure 3b shows the adsorption curves in wet conditions for five individual PD runs. It is noted that these adsorption curves are less consistent than those obtained from CB due to a series of random, stepwise

(46) Savitzky, A.; Golay, M. J. E. *Anal. Chem.* **1964**, *36*, 1627.

(47) Luo, J. W.; Ying, K.; He, P.; Bai, J. *Digital Signal Process.* **2005**, *15*, 122.

(48) Lide, D. R. *CRC Handbook of Chemistry and Physics*, 85th ed.; CRC Press: Boca Raton, FL, 2004.

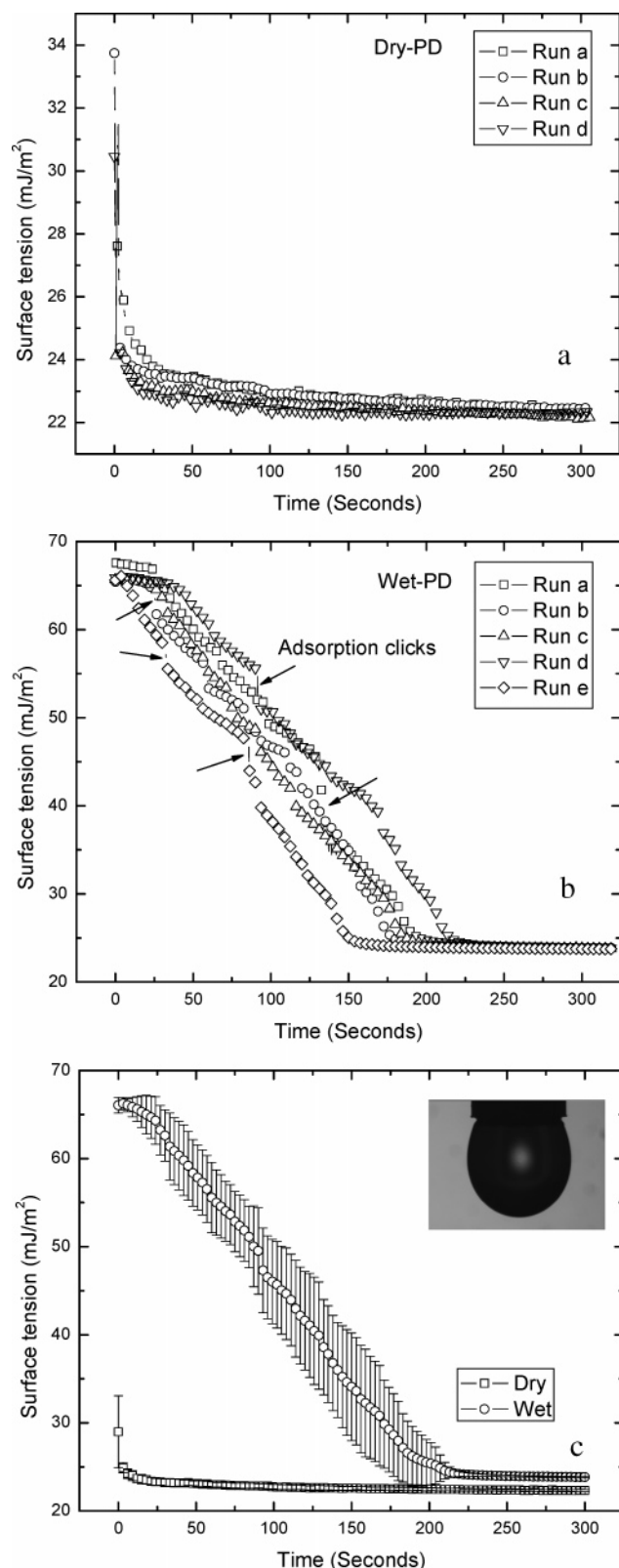


**Figure 3.** Dependence of adsorption kinetics of 0.5 mg/mL BLES on humidity, studied by a pendant drop (PD) method at 37 °C. (a) Four individual experimental runs in dry conditions; (b) five individual experimental runs in wet conditions, where some “adsorption clicks” are indicated by the arrows; (c) averaged adsorption curves in dry and wet conditions. The error bar shows the standard deviation of the average.

surface tension drops occurring within very short periods (<0.2 s). These sudden decreases in surface tension have been observed before<sup>25,49</sup> and were referred to as “adsorp-

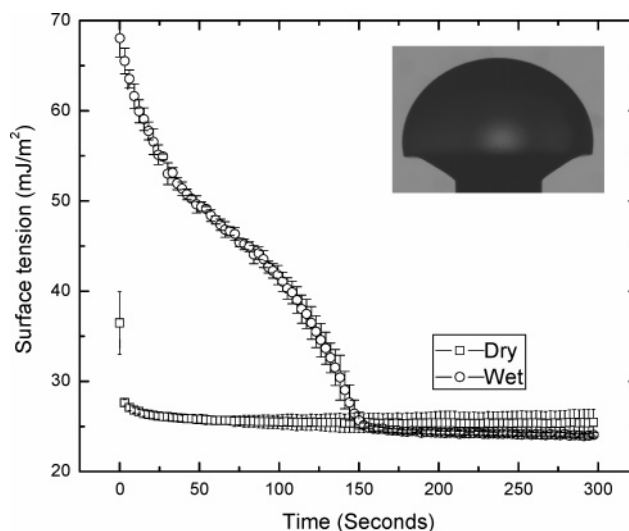


**Figure 4.** Dependence of adsorption kinetics of 0.5 mg/mL BLES on humidity, studied by a constrained sessile drop (CSD) method at 37 °C. Each curve is averaged from at least three individual experimental runs. The error bar shows the standard deviation of the average.

tion clicks”.<sup>49</sup> Because of these adsorption clicks, the individual adsorption curves obtained from PD are locally diverse. It is also noted that the adsorption clicks generally occur at a surface tension above 40 mJ/m<sup>2</sup>. This is also consistent with previous observations.<sup>25</sup>

Figure 3c shows the comparison of the averaged adsorption curves (from those shown in Figure 3, panels a and b, respectively) in dry and wet conditions. It is noted that, due to adsorption clicks, the error associated with the average of PD results is much larger than that of CB (Figure 2c). However, similar to CB, results from PD also suggest a significant effect of humidity on the adsorption rate of BLES.

**3.3. CSD Studies.** Adsorption curves obtained from CSD in dry and wet conditions also show good reproducibility (results not shown) and are similar to those obtained from CB. Figure 4 compares the averaged adsorption curves (each from at least three individual runs) in dry and wet conditions. Again, the adsorption curve in dry conditions shows a faster decrease, consistent with the curves obtained from CB and PD. In addition, in wet conditions, a shoulder also appears at surface tensions around 40 mJ/m<sup>2</sup>, similar to that observed from CB.

**3.4. Summary of the Experimental Results. 3.4.1. Dynamic Surface Tension.** The results obtained from the three experimental arrangements (Figures 2c, 3c, and 4) are summarized in Table 1. The first four columns in Table 1 show the surface tensions at the onset of the experiment ( $\gamma_0$ ), and after 50 ( $\gamma_{50}$ ), 100 ( $\gamma_{100}$ ), and 300 s ( $\gamma_{300}$ ). It is clear that in dry conditions  $\gamma_0$  is less than 37 mJ/m<sup>2</sup>, far less than the surface tension of a clean air–water interface (i.e., ~70 mJ/m<sup>2</sup>). In comparison,  $\gamma_0$  measured in wet conditions is closer to 70 mJ/m<sup>2</sup>.

A  $\gamma_0$  value lower than that of a clean air–water interface indicates preadsorption occurring during formation of the drop/bubble, which cannot be followed by the present experimental methodologies. The extent of preadsorption is a function of the amount of surfactant molecules available to preadsorb (i.e., the surfactant concentration and the sample size) and the time allowed for preadsorption (i.e., the time used to form a drop/bubble). For each

(49) Schürch, S.; Schürch, D.; Curstedt, T.; Robertson, B. *J. Appl. Physiol.* **1994**, *77*, 974.

**Table 1. Critical Surface Tensions and Time Scales for the Adsorption of 0.5 mg/mL BLES under Dry and Wet Conditions<sup>a</sup>**

humidity	setups	$\gamma_0^b$ (mJ/m <sup>2</sup> )	$\gamma_{50}^b$ (mJ/m <sup>2</sup> )	$\gamma_{100}^b$ (mJ/m <sup>2</sup> )	$\gamma_{300}^b$ (mJ/m <sup>2</sup> )	$t_{50}^c$ (s)	$t_{95}^c$ (s)
dry	CB	31.1	24.8	24.6	24.5	0 <sup>d</sup>	10.2
	PD	29.0	23.1	22.7	22.3	0 <sup>d</sup>	4.2
	CSD	36.5	25.8	25.5	25.5	0 <sup>d</sup>	3.0
wet	CB	56.7	47.0	40.5	24.2	46.6	171
	PD	66.1	58.0	45.9	23.8	95.6	190
	CSD	66.5	47.7	38.1	24.0	52.7	146

<sup>a</sup> Results are obtained from three different experimental arrangements, i.e., CB, PD, and CSD, at 37 °C. <sup>b</sup>  $\gamma_0$ ,  $\gamma_{50}$ ,  $\gamma_{100}$ , and  $\gamma_{300}$  are the surface tensions at the onset of the recording, after 50, 100, and 300 s, respectively. <sup>c</sup>  $t_{50}$  and  $t_{95}$  are the time intervals for dynamic surface tension to decrease by 50 and 95% of its total decrease from the surface tension of a fresh air–water interface (i.e., 70.1 mJ/m<sup>2</sup> at 37 °C) to the equilibrium surface tension of a predominantly phospholipid film (indicated by  $\gamma_{300}$ ). <sup>d</sup> A time of zero means that  $t_{50}$  is reached before the time to start recording images, i.e., within the interval of forming the drop/bubble, which is generally less than 5 s for all of the three different arrangements.

experimental arrangement, the times used to form a drop/bubble in dry and wet conditions are the same. Therefore, the significant difference in  $\gamma_0$  in dry and wet conditions, demonstrated by each experimental setup, can be only due to the humidity.

In dry conditions,  $\gamma_{50}$  measured by all three methods is already close to the equilibrium values (i.e., 22–25 mJ/m<sup>2</sup>). In contrast,  $\gamma_{50}$  and even  $\gamma_{100}$ , in wet conditions are well above the equilibrium values.  $\gamma_{300}$  measured by all three arrangements, in both dry and wet conditions, is very close and within the range of the equilibrium values, suggesting that humidity does not change the equilibrium surface tension of the lung surfactant.

The last two columns in Table 1 show two time scales commonly used to measure the kinetics of an adsorption process.  $t_{50}$  and  $t_{95}$  are respectively the time scales for the DST to drop by 50 and 95% of its total decrease from the air–water value (i.e., 70.1 mJ/m<sup>2</sup> at 37 °C) to the equilibrium value (indicated by  $\gamma_{300}$ ). It should be noted that  $t_{50}$  is zero for the three arrangements for measurements in dry conditions. This means that a 50% decrease of surface tension is essentially completed before the onset of taking images, i.e., time zero. In contrast,  $t_{50}$  in wet conditions is generally above 45 s.  $t_{95}$  measured in dry condition is generally less than 11 s. In contrast, in wet conditions,  $t_{95}$  is generally 20-fold greater.

**3.4.2. Adsorption Rate.** Detailed study of the adsorption kinetics requires the investigation of the adsorption rate, i.e., the first derivative of surface tension decrease with time ( $-d\gamma/dt$ , mJ/(m<sup>2</sup>s)). In dry conditions, the adsorption occurs so fast that our methods cannot follow the initial decrease of surface tension. Therefore, only the adsorption rate in wet conditions is reported. Figure 5a shows the curves of the adsorption rate, calculated from the averaged curves of dynamic surface tension shown in Figures 2c, 3c, and 4, respectively, as a function of time obtained by CB, PD, and CSD in wet conditions. It is noted that the curve obtained by PD shows a pattern different from those by CB and CSD. The curves from CB and CSD show a similar sigmoid pattern. The adsorption rate first decreases to a minimum and then increases to a local maximum. After that, the adsorption rate decreases again to zero. However, the curve for PD lacks the initial decrease of the adsorption rate, as observed in CB and CSD. The adsorption rate in PD increases first to a maximum and then decreases to zero.

It is also noted that, even though sharing the same pattern, the metastable points in the curves obtained from

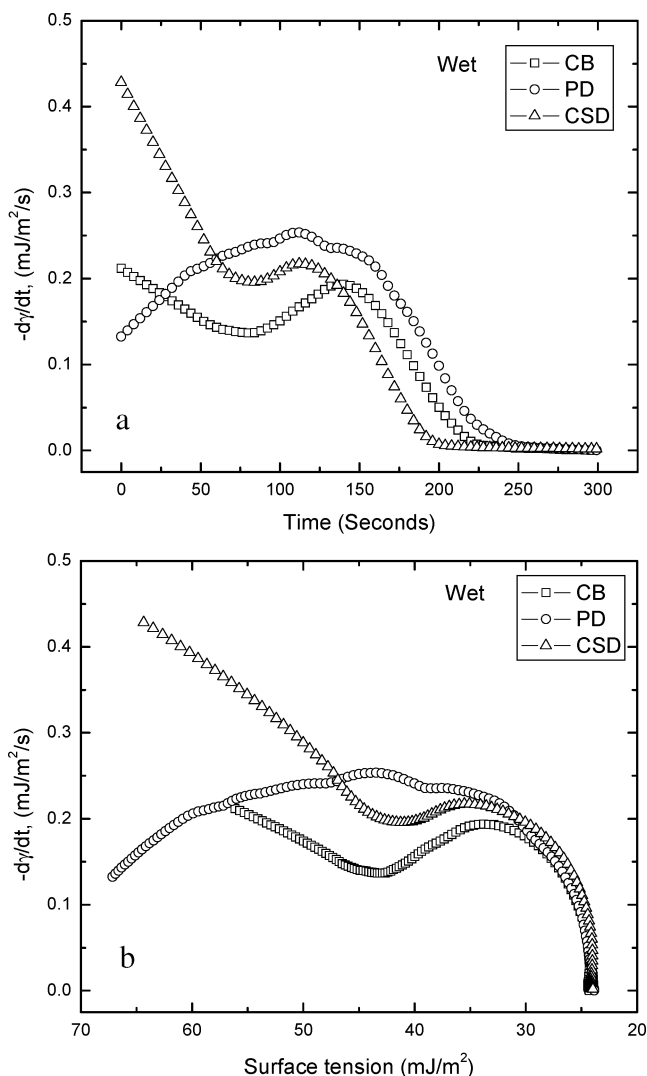


**Figure 5.** Rate of adsorption ( $-d\gamma/dt$ , mJ/(m<sup>2</sup>s)) of 0.5 mg/mL BLES in wet conditions at 37 °C (a) as a function of adsorption time; (b) as a function of surface tension.

CB and CSD shift up to 30 s on the abscissa (Figure 5a). Figure 5b replots the adsorption rates in wet conditions against the surface tension. It can be seen that the metastable points in the curves from CB and CSD coincide with each other very well. A local minimum of the adsorption rate occurs at surface tensions of 40–45 mJ/m<sup>2</sup>; a local maximum occurs at 30–35 mJ/m<sup>2</sup>. The adsorption rate measured from PD only shows a local maximum, at a surface tension of 40–45 mJ/m<sup>2</sup>.

#### 4. Discussion

The effect of humidity on the adsorption kinetics of lung surfactant has been largely disregarded in previous in vitro studies. In CB experiments, ambient air was usually used to form the bubble.<sup>42,49</sup> In PD/CSD experiments, the atmosphere in the drop chamber was carefully saturated with water to eliminate drop evaporation<sup>24,25,45</sup>. Under these circumstances, a distinct difference in the adsorption kinetics of BLES was found between the bubble and drop methods. That is, at the same concentration (e.g., 0.5 mg/mL BLES) adsorption in a CB arrangement was much more rapid than that in the drop arrangements. However, after careful evaluation and control of the humidity, the three different experimental arrangements yield similar results (Figures 2–4). Therefore, our experimental results strongly suggest a common dependence of the adsorption

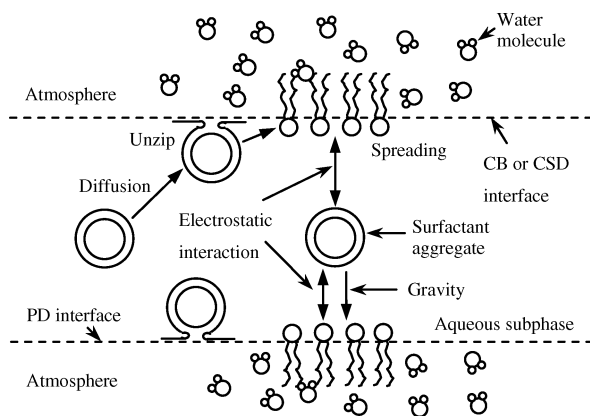


**Figure 6.** Schematic of the adsorption models in captive bubble (CB), pendant drop (PD), and constrained sessile drop (CSD).

kinetics of BLES on humidity, i.e., 100% RH at 37 °C slows down the adsorption compared with the lower humidity. Analysis shows that our experimental results agree well with an adsorption model considering the combined effects of entropic force, electrostatic interaction, and gravity, as discussed below. These results may also shed light on understanding the rapid adsorption of lung surfactant in vivo.

**4.1. Effect of an Entropic Barrier Due to the High Humidity.** Lung surfactant in vivo and in vitro exists as a variety of molecular aggregates including unilamellar and multilamellar vesicles and tubular myelin.<sup>50</sup> Adsorption of these phospholipid aggregates from the aqueous dispersion to the air–water interface likely consists of two sequential steps (see Figure 6 for a schematic).<sup>14,15,17,18,22,51</sup> First, the phospholipid aggregates must diffuse to and contact the interface from the aqueous subphase closely adjacent to the interface. Subsequently, these aggregates have to “unzip” and spread on the interface, thus forming an insoluble surfactant monolayer or a multilayer structure, the so-called “surface-associated reservoir”.<sup>52</sup>

Unzipping and spreading of the phospholipid aggregates at the air–water interface need to overcome a thermodynamic barrier.<sup>17</sup> The major contribution to this thermodynamic barrier arises from an unfavorable entropy change during the unravelling of these aggregates and the exposing of the hydrophobic phospholipid fatty acid chains to the atmosphere.<sup>18,51</sup> The entropic barrier encountered by this transition could be substantially increased if the water vapor in the atmosphere had a sufficiently high concentration, e.g., for the case of 100% RH at 37 °C. Both Colacicco et al.<sup>33</sup> and Wildeboer-Venema<sup>34</sup> found that a 100% RH played a role in decreasing film stability only at 37 °C but not at room temperature. This is consistent with the present adsorption results from CB, where we injected a bubble at 25 °C and 50% RH. No inhibiting effect on adsorption has been found (Figure 2a). The saturation vapor pressures at 25 and 37 °C are 3.29 and 6.44 kPa,<sup>48</sup> respectively. Therefore, our CB results imply that only a high concentration of water vapor can increase the entropic barrier to such an extent that it is able to slow adsorption. Even though the vapor pressure at which the inhibiting effect becomes significant is not known, 100% RH at 37 °C, i.e., 6.44 kPa in vapor pressure, definitely shows the inhibiting effect.

**4.2. Effect of Electrostatic Interaction and Gravity.** Schram and Hall<sup>18</sup> found that the adsorption kinetics of lung surfactant generally shows three stages: an initial delay during which surface tension remains constant, followed by a decrease of surface tension to approximately 40–45 mJ/m<sup>2</sup> at decreasing rates, and a subsequent acceleration of the rate of surface tension decrease before reaching the equilibrium value of approximately 25 mJ/m<sup>2</sup>. The lag time prior to the initial surface tension decrease strongly depended on the surfactant concentrations and the presence of surfactant proteins.<sup>18</sup> For BLES at the concentration tested here, i.e., 0.5 mg/mL, the initial lag phase is expected to be undetectably short.<sup>18</sup> In our experiments, the other two phases of the adsorption kinetics are observed by the CB and CSD in wet conditions but not by the PD. In dry conditions, the adsorption is always too rapid to be followed by the current methodology. Therefore, only the adsorption in wet conditions is discussed here.

For CB and CSD, the adsorption rate clearly shows the early decrease and the subsequent increase at surface tensions near 40–45 mJ/m<sup>2</sup>, followed by a second decrease, initiated at 30–35 mJ/m<sup>2</sup>, to the equilibrium (Figure 5b). For the first stage of initial decrease in the adsorption rate, entropy is the main rate-limiting thermodynamic factor and the rate is mainly controlled by the subphase concentration.<sup>18</sup> During this stage, the surfactant aggregates diffuse to and spread onto the originally clean interface. This process progressively slows down as the phospholipid density on the surface rises.

For the second stage, i.e., the increase in the adsorption rate, mechanisms other than simple accumulation of surfactant molecules on the surface play a role. Walters et al.<sup>17</sup> and Ross et al.<sup>15</sup> found that the addition of anionic phospholipids, such as DPPG, can accelerate the adsorption of surfactant protein-DPPC vesicles no matter whether the DPPG is located in the prespread interfacial film or in the aqueous subphase. They attributed this promotion of adsorption to a reduced adsorption barrier encountered by neutral vesicles, by introducing electrostatic interactions.<sup>15,17</sup>

Lung surfactant adsorption shares a number of characteristics with bilayer fusion in which the flattening and merging of two approaching bilayers are opposed by the repulsive hydration and/or entropic forces.<sup>53,54</sup> Recent studies<sup>15,17,55–58</sup> suggest that these repulsive forces stabilizing a lung surfactant dispersion can be counteracted by electrostatic interactions between the positively charged surfactant proteins (e.g., SP-B and SP-C) and the negatively charged anionic phospholipids (e.g., PGs). As a result, SP-B and SP-C facilitate rapid adsorption and reinsertion of the phospholipid vesicles into the interfacial film after film collapse.<sup>58</sup>

It is noted that the increase of the adsorption rate starts at surface tensions of 40–45 mJ/m<sup>2</sup>, for both the CB and CSD arrangements (Figure 5b). These surface tensions may indicate that the adsorbed film has reached a threshold surface concentration of anionic phospholipids (mainly PG compounds) large enough to induce a pronounced electrostatic attractive force to promote adsorp-

(50) Schürch, S.; Green, F. H. Y.; Bachofen, H. *Biochim. Biophys. Acta* **1998**, *1408*, 180.

(51) King, R. J.; Clements, J. A. *Am. J. Physiol.* **1972**, *223*, 727.

(52) Schürch, S.; Qanbar, R.; Bachofen, H.; Possmayer, F. *Biol. Neonate* **1995**, *67*, 61.

(53) Leikin, S.; Parsegian, V. A.; Rau, D. C.; Rand, R. P. *Annu. Rev. Phys. Chem.* **1993**, *44*, 359.

(54) Israelachvili, J.; Wennerstrom, H. *Nature* **1996**, *379*, 219.

(55) Rodriguez-Capote, K.; Nag, K.; Schürch, S.; Possmayer, F. *Am. J. Physiol. Lung Cell Mol. Physiol.* **2001**, *281*, L231.

(56) Pérez-Gil, J. *Biol. Neonate* **2002**, *81* (suppl 1), 6.

(57) Cruz, A.; Vazquez, L.; Velez, M.; Pérez-Gil, J. *Biophys. J.* **2004**, *86*, 308.

(58) Alig, T. F.; Warriner, H. E.; Lee, L.; Zasadzinski, J. A. *Biophys. J.* **2004**, *86*, 897.

tion (see Figure 6 for a schematic). When surface tension is lower than 40–45 mJ/m<sup>2</sup>, the adsorption rate is dependent more on the interfacial concentration of the film than the subphase concentration. When surface tension decreases to 30–35 mJ/m<sup>2</sup>, the surface concentration has reached such a high level that further adsorption will be slow. Consequently, the adsorption rate decreases gradually to zero, indicating equilibrium. It should also be noted that we cannot exclude other mechanisms, e.g., the squeeze-out of the hydrophobic surfactant proteins,<sup>59,60</sup> or phase transition/separation, happening in this surface tension range, which may also play a role in changing the adsorption rate.

The adsorption rate for PD is different from those for CB and CSD in that no early decrease is observed (Figure 5, panels a and b). In addition, individual curves of DST obtained from PD (Figure 3b) are different from the others in that numerous adsorption clicks appear. These differences in the adsorption behavior between PD and CB/CSD may imply that gravity plays a role in the adsorption of lung surfactant aggregates, especially in the first step, i.e., the moving of the surfactant aggregates to the interface (see Figure 6 for a schematic). Adsorption clicks imply a quick and cooperative movement of large flakes of aggregated surfactant molecules into the air–water interface.<sup>49</sup> By further assuming aggregates of pure DPPC, Schürch et al.<sup>49</sup> estimated that the lung surfactant aggregates correspond to particles with a diameter of ~3 μm. PD differs from the other two configurations in that gravity turns to push large surfactant aggregates toward the surface. The air–water interface of PD is located at the bottom of the surfactant subphase; in contrast, the interfaces of CB/CSD are located at the top, similar to those in a Langmuir trough and pulsating bubble surfactometer. The lack of initial decrease in the adsorption rate for PD could also indicate that gravity initially enhances adsorption.

In addition, previous<sup>25,49</sup> and present (Figure 3b) studies found that significant adsorption clicks only occur at surface tensions above 40 mJ/m<sup>2</sup>. Thereafter, at lower surface tensions, the interface is largely covered by surfactant molecules, thus blocking further access of large aggregates. This threshold surface tension of 40 mJ/m<sup>2</sup> makes sense since it coincides with the local maximum in the curve of the adsorption rate (Figure 5b), where the effect of increased surface concentration starts to outweigh the effects of gravity and electrostatic attraction on adsorption. Consequently, the adsorption rate starts decreasing.

**4.3. Physiological Implication.** It is well-known that the alveolar gas is saturated with water.<sup>36,37</sup> Before arriving at the lungs, the inspired air is continuously humidified when passing through conducting airways to achieve a core temperature of 37 °C and 100% RH.<sup>37</sup> Thus, in the lungs, the deleterious effect of 100% RH found here must be counteracted by some mechanisms to ensure rapid adsorption. Several mechanisms might be involved as follows.

First, the effect of 100% RH can be overcome by high surfactant concentrations. As shown before,<sup>25</sup> BLES at physiologically relevant concentrations (i.e., >3 mg/mL) adsorbed rapidly to the surface of a PD in a water-saturated chamber. These results suggest that high phospholipid concentrations, occurring in the lungs, help

to overcome the effect of humidity, thus ensuring rapid adsorption *in vivo*.

Second, SP-A could play a role in enhancing adsorption kinetics *in vivo*. SP-A is absent from all of the commercial therapeutic lung surfactant currently available, including BLES, i.e., the preparation used here. It has been shown before that adsorption of 0.5 mg/mL complete natural surfactant (i.e., at the same concentration used here) is very fast in a water-saturated chamber.<sup>24</sup> This suggests that SP-A may be responsible for counteracting the effect of humidity *in vivo*. Thermodynamic analysis for the adsorption processes of complete natural surfactant (with SP-A) and surfactant extracts (without SP-A) showed very different rate-limiting factors, thus suggesting distinct mechanisms for their adsorption.<sup>18</sup> SP-A can promote the formation of tubular myelin by phospholipid–protein interactions.<sup>5,61</sup> Tubular myelin is highly surface active and most likely represents an immediate precursor of the lung surfactant film at the air–water interface of alveoli.<sup>5</sup> By forming tubular myelin structures, the complete natural surfactant could cause rapid adsorption without being impeded by the 100% RH *in vivo*.

Third, the adsorption of endogenous surfactant from the hypophase of the alveolar lining layer appears to be affected by several factors, such as pH, ionic strength of the hypophase, and composition of the alveolar gas. Colacicco et al.<sup>33</sup> found that low pH (i.e., <6.5) can help resist the effect of 100% RH on destabilizing the DPPC films. They speculated that a lower pH moderates the repulsive forces between the polar headgroups of DPPC molecules and therefore favors tight compaction of the film. More recent studies<sup>29–31</sup> also confirmed the effect of pH on the adsorption kinetics of surfactant preparations lacking SP-A. Increasing pH impedes adsorption. Camacho et al.<sup>31</sup> suggested that an alkaline pH inhibits the surface activity of lung surfactant by impairing the electrostatic interactions between the positively charged hydrophobic proteins and the anionic phospholipids. However, the addition of SP-A is able to resist the effect of alkaline pH by providing additional charge.<sup>29,30</sup>

The effect of pH could also be compensated for by altering the ionic strength of the electrolyte solutions<sup>28,32</sup> and the composition of the gas exposed to the surfactant film.<sup>35</sup> It was found that the ionic strength affects the adsorption kinetics in a similar way as pH, i.e., by modulating the electrostatic forces between the film and the surfactant aggregates.<sup>28,32</sup> The effect of gas composition was first considered by Wildeboer-Venema,<sup>35</sup> who found that a gas phase containing carbon dioxide can counteract the effect of humidity. He attributed this beneficial effect of CO<sub>2</sub> to its ability to decrease subphase pH. The alveolar gas features a high content of carbon dioxide (i.e., ~40 mmHg) compared to air (i.e., ~0.4 mmHg).<sup>37</sup> Therefore, there is a possibility that CO<sub>2</sub> alters the surface properties of the adsorbed lung surfactant films *in vivo* to overcome the effect of 100% RH.

## 5. Conclusions

Our experimental results clearly demonstrate impaired adsorption kinetics due to 100% RH at 37 °C. This is attributed to an increased entropic barrier due to the addition of water molecules in the gas phase when the phospholipid aggregates unzip and spread at the air–water interface. Further analysis of the adsorption rate and adsorption clicks suggests different film formation mechanisms for the PD and CB/CSD methods. For all

(59) Wüstneck, N.; Wüstneck, R.; Fainerman, V. B.; Miller, R.; Pison, U. *Colloids Surf. B: Biointerfaces* **2001**, *21*, 191.

(60) Wüstneck, R.; Wüstneck, N.; Moser, B.; Pison, U. *Langmuir* **2002**, *18*, 1125.

(61) Suzuki, Y.; Fujita, Y.; Kogishi, K. *Am. Rev. Respir. Dis.* **1989**, *140*, 75.

three arrangements, both electrostatic interaction and gravity play a role in the adsorption of lung surfactant aggregates. However, gravity works in opposite directions for PD and CB/CSD.

It is apparent that carefully considering and maintaining a 100% RH at 37 °C are important to the in vitro evaluation of surfactant function and the performance of surfactant replacement formulations. In particular, a captive bubble will not have 100% RH if ambient air is used to form the bubble. Further characterization of the underlying mechanisms of lung surfactant adsorption under physiological conditions requires the understanding

of the specific interaction/binding between the primary phospholipid components, such as PCs, PGs, and the surfactant associated proteins.

**Acknowledgment.** This work was supported by a grant from Canadian Institutes of Health Research (MOP-38037) and an Open Fellowship from University of Toronto to Y.Y.Z. We also thank Dr. David Bjarneson of BLES Biochemicals Inc. for his generous donation of the BLES samples.

LA0517078